Proceeding of the IEEE
International Conference on Robotics and Biomimetics
Dali, China, December 2019

A Single Driven Bionic Water Strider Sliding Robot Mimicking the Spatial Elliptical Trajectory*

Jihong Yan, Xin Zhang, Kai Yang, Jie Zhao, *Member, IEEE*

***Abstract*—When a water strider sliding on the water, the spatial elliptical trajectory of the driving leg plays a critical role in ensuring efficient sliding movement and stability. At present, the bionic water strider robot prototype generally adopts the dual motor drive mode to realize this complex spatial trajectory, increasing the weight of the robot and go against the maximization of the performance. Moreover, the research on bionic water strider robots mainly focuses on the tiny scales, the load capacity is weak, and difficult to achieve practical application. In response to these problems, this paper proposes a new driving principle, the driving leg realizes the spatial elliptical trajectory by the elliptical slot cam and the two rotating mechanisms driven by a single motor. Based on this, a small water surface sliding robot based on buoyancy support is designed. In order to verify the motion performance of the robot, the dynamic model was established. Then, ADAMS and MATLAB co-simulation method was adopted to analyze the sliding movement of the robot. Finally, the forward and turning motion experiments of the robot prototype with different stroke speeds were conducted. The total weight of the robot is 137g, with an additional load capacity of 130g, the maximum straight stroke speed of the robot is 24.3cm/s, and the maximum turning speed is 35°/s.**

I. INTRODUCTION

The water strider is capable of sliding quickly and flexibly without penetrating the water surface, which is a desired bionic object for water surface motion robots due to the small sliding resistance and high efficiency, the driving leg of water strider has a spatial elliptical trajectory when sliding on the water. For the moment, bionic water strider robots can be divided into two categories: surface tension-driven robots and hydrodynamic pressure-driven robots according to driving mechanism, the former focuses on the motion mechanism of water strider[1-5], which has a light weight and small scale with weak load capacity, the latter focuses on the motion trajectory imitation of water strider, which has larger weight and size than the former's and has the load capacity to carry sensors to adapt more complex water environment[6-10]. As a consequence, research on the hydrodynamic pressure-driven robots is more conducive to practical applications.

*Research supported by Natural Science Foundation of China (NSFC, Grant 5177513).

Jihong Yan is with State Key laboratory of Robotics and Systems, Harbin Institute of Technology, Harbin 150001, P. R. China (corresponding author to provide phone: 86-451-86413392; fax: 86-451-86413392; e-mail: jhyan@hit.edu.cn).

Xin Zhang, Kai Yang and Jie Zhao are with State Key laboratory of Robotics and Systems, Harbin Institute of Technology, Harbin 150001, P. R. China

In order to vividly imitate the sliding motion of water strider, driving legs of bionic water strider robots should have the spatial elliptical trajectory like water strider's. Therefore, domestic and foreign scholars have carried out a lot of research work and developed a series of bionic water strider sliding robots. In 2005, the bionic water strider sliding robot developed by Chuo University realized the spatial elliptical sliding trajectory by combining the direct drive of the motor and the parallel four-bar linkage mechanism[9]. In 2012, Hebei University of Technology developed a water surface sliding robot, realizing the spatial motion trajectory by the crank rocker and the parallel four-bar linkage with two motors for a driving leg[11]. In 2016, the bionic water strider sliding robot developed by Zhejiang University was driven by two motors in series, realizing the spatial elliptical sliding trajectory of the driving legs [12]. In a word, the driving legs of the hydrodynamic pressure-driven robots realize the spatial elliptical sliding trajectory with two motors, increasing the weight of the robot and reducing the motion performance of the robot, which is not conducive to the application development of the robot.

This paper proposes a new type of bionic water strider sliding robot based on the cam driving mechanism, and carries out research on the motion performance of the robot when sliding on the water surface. Section II introduces driving mechanism and the overall structural design of the robot. In section III, forces of the supporting legs and driving legs are analyzed carefully, on this basis, the robot dynamics model is established, and analyze the motion performance of the robot by co-simulation of MATLAB and ADAMS. Finally, the forward and turning motion experiments of the robot prototype at different sliding speeds are carried out to verify the validity of the simulation.

II. ROBOT DESIGN

A. Driving mechanism

Water strider has the ability to slide on the water surface sensitively without penetrating the water, this is because the surface tension generated by the front and hind legs of water strider provides sufficient supporting force. The driving force of the sliding movement is mainly caused by the dynamic pressure generated by the rapid stroke of the driving legs. Fig. 1 denotes the movement trajectory of the driving legs, the green curve indicates the sliding process of the driving leg under water surface, while the blue curve represents the swinging process of the driving leg above the water surface. The sliding trajectory of the driving leg is approximately a spatial ellipse. The stroke movement can be divided into three

978-1-7281-6321-5/19//$31.00 ©2019 IEEE

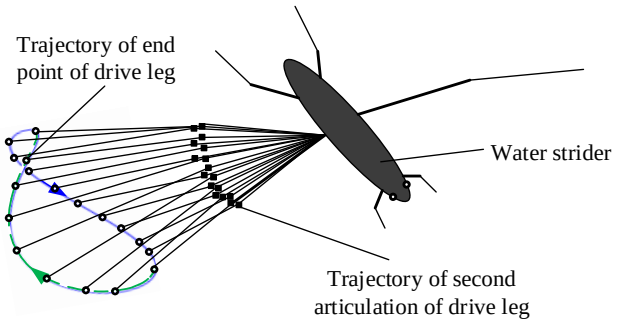

Fig. 1.Trajectory of the driving legs.

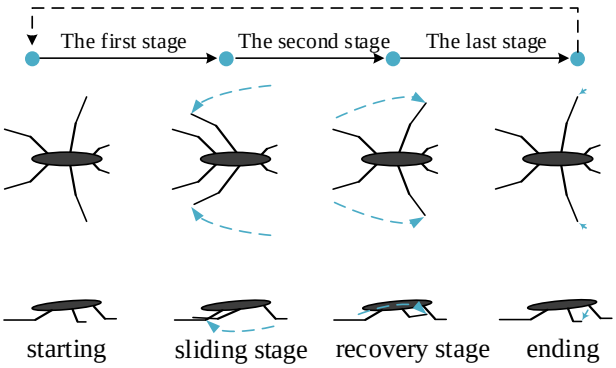

Fig. 2. Straight sliding movement of water strider.

stages during the straight sliding movement as shown in Fig. 2, the driving leg sliding backwards swiftly to generate driving force in the sliding stage. Then, the driving leg leaves the water surface and the water strider continues to move on the surface due to inertia. In the final stage, the driving leg moves to the initial position to prepare for the next sliding cycle.

In order to imitate the spatial elliptical sliding trajectory of water strider, this paper proposes a new driving mechanism, each driving leg realizes the spatial elliptical sliding trajectory by a single motor, which reduces the weight of the driving mechanism and improves the motion performance of the robot. The robot acquires the plane elliptical motion trajectory with slot cam, and obtains the spatial elliptical motion trajectory with telescopic lever mechanism, the driving principle diagram is illustrated in Fig. 3. When the crank *AB* rod rotates,

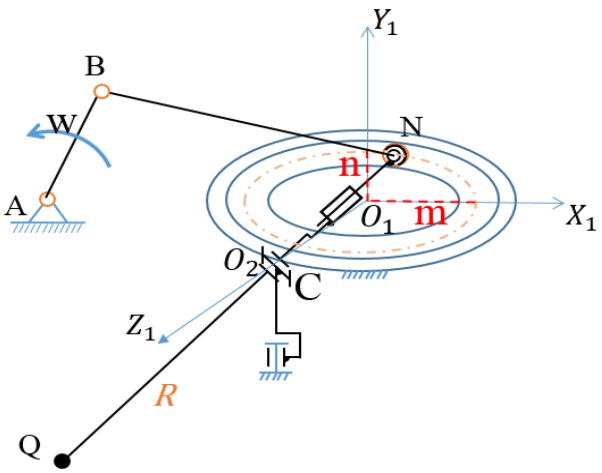

Fig. 3. The drive mechanism schematic.

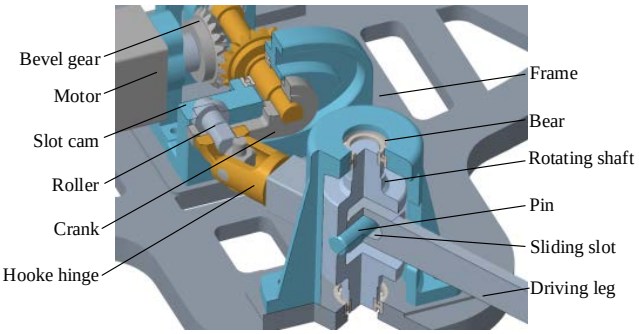

Fig. 4. The drive mechanism diagram.

the point *N* is driven to move inside the elliptical slot cam. The point *N* represents the ball hinge, which is connected to the point *C* by the telescopic lever mechanism, the point *C* and *Q* represents the spatial orthogonal two DOF rotation fulcrum and the endpoint of driving leg respectively, the plane elliptical motion trajectory of the ball hinge is mapped to the spatial elliptical trajectory of the endpoint of driving leg through the *CQ* rod. Appropriate adjustment of the above-mentioned driving principle is required when designing the robot drive mechanism: in order to make the drive mechanism more compact, the crank slider mechanism should be replaced with the guide rod slider mechanism, considering the difficulty in processing and installation of the ball hinge, replace it with the Hooke hinge. The driving mechanism of the robot is shown in Fig. 4.

The robot drives the crank through the bevel gear with a DC geared motor, and drives the roller to move inside the elliptical slot cam, the roller is connected to the driving leg through the Hooke hinge. Two brackets with two orthogonal rotational DOF are mounted on both sides of the robot, and there is a sliding slot inside the driving leg, which is connected to the bracket through this sliding slot. Under the constraint of the plane elliptical motion trajectory of the roller, the endpoint of the driving leg possesses a spatial elliptical motion trajectory. When the paddle moves to the lower part of the spatial elliptical trajectory, the paddle is in contact with the water and generates driving force to make the robot move forward. When the paddle moves to the upper part of the spatial elliptical trajectory, the paddle is separated from the water surface, and the robot will decelerate under the resistance of the supporting legs until the paddle contact the water to generate the driving force.

B. Supporting legs design

The distance between two front supporting legs of water strider are smaller compared to the distance between two hind supporting legs, the design of the supporting legs of the robot is consistent with this layout. In order to ensure that the designed robot has enough load capacity, the robot adopts four hollow ellipsoids as supporting legs arranged symmetrically to increase the total volume of the support legs and decrease the weight of the robot.

Fig. 5 illustrates the force model of the hollow ellipsoidal supporting legs on water surface. In the figure, the water surface is defined as the *X* axis, the direction perpendicular to the water surface and screen are chosen as the *Y* axis and *Z*

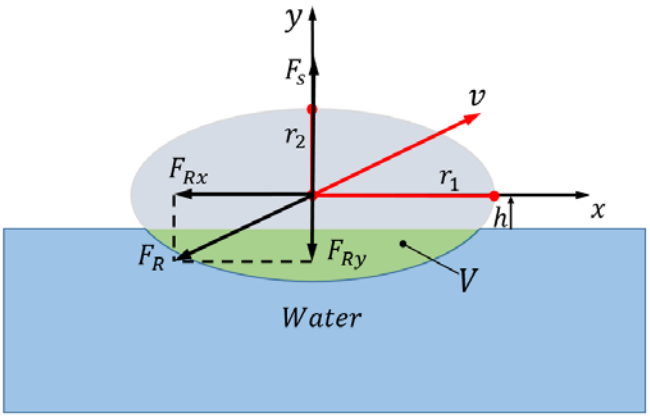

Fig. 5. Forces exerted on the supporting legs

$$F_s = \begin{cases} 0 & h \geq r_2 \\ \pi\rho_w g r_1 r_2 \left(\frac{h^3}{3r_2^2} + \frac{2}{3}r_2 - h\right) & -r_2 < h < r_2 \\ \frac{4}{3}\pi\rho_w g r_1 r_2^2 & h \leq -r_2 \end{cases} \quad (1)$$

axis separately, the buoyance force of each supporting leg can be calculated by Equation (1). Where h is the submerged depth of the center of the hollow ellipsoidal supporting leg, ρ_w is the density of water, so the buoyancy force is defined as a function of submerged depth of the center of the ellipsoidal leg. If h is larger than r_2, the robot don't contact with the water, the buoyancy force is zero, if h is smaller than $-r_2$, the supporting leg is totally submerged under the water and the buoyancy achieves the maximum. If $h \in (-r_2, r_2)$, the buoyancy force is calculated by the submerged crown volume. When r_1 is 40mm, r_2 is 20mm, the buoyancy obtained is about 2.68N, and the weight of the robot designed is about 1.3N, so that even if the prototype is tilted due to water fluctuation in the sliding process, the robot can still obtain sufficient lifting force to keep stable on the water surface.

C. Robot prototype

The bionic water strider sliding robot was fabricated as shown in Fig. 6. It mainly consists of the frame, four supporting legs, two driving legs and drive mechanisms, the

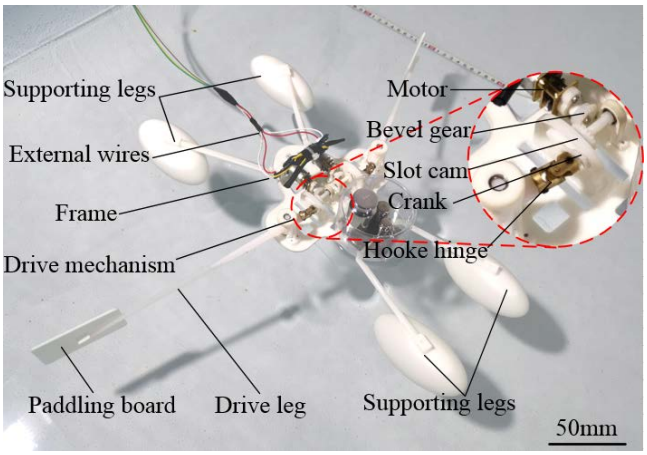

Fig. 6. Bionic water strider sliding robot

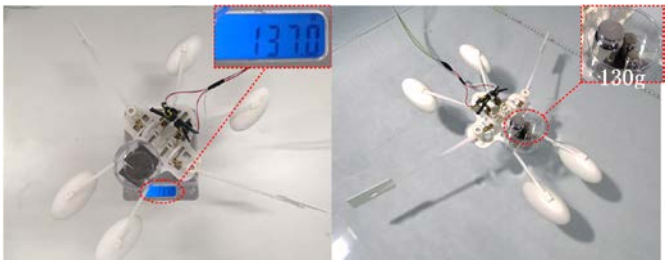

Fig. 7. The weight and load capacity of the robot

drive mechanism is composed of motor, bevel gears, slot cam, crank, and Hooke hinge, each of driving leg is fixed on the Hooke hinge of the drive mechanism driven by a DC motor through the slot cam. The robot weighs 137g and its total length, width and height are 394mm, 330mm and 70mm respectively. The load capacity is 130g, as shown in Fig. 7. The main frame, slot cam driving legs and supporting legs are manufactured by 3D printing techniques to reduce the robot's weight, and the supporting legs are treated with hydrophobic material to reduce drag force during the sliding process.

III. Force Model and Dynamic Analysis

A. Force model

The driving leg has a spatial elliptical sliding trajectory when the robot sliding on the water surface. To simplify the movement process, the trajectory of the driving leg is projected in the horizontal plane, ignoring the change of the projection radius caused by the spatial elliptical trajectory. As shown in Fig. 8, the swinging range of the driving leg is 2α in the horizontal plane, C_d indicates the flow resistance coefficient of the driving leg, which reflects the influence of the shape and size of the driving leg on sliding movement and the value is 0.8 in this paper, v_{xz} and v_{xz1} indicate the horizontal projections of the speed of the driving leg relative to the robot frame and water respectively, and β is the angle between them, v_d indicates the velocity of the robot, θ indicates the angle between the driving leg and the Z-axis of the robot, and S indicates the area of the driving leg under the water surface. The driving force F_q of a single driving leg is illustrated in Equation (2). When the X-axis of the ellipsoidal supporting leg coincides with the movement direction of the robot, the resistance F_{Rx} in the forward direction for each support leg is

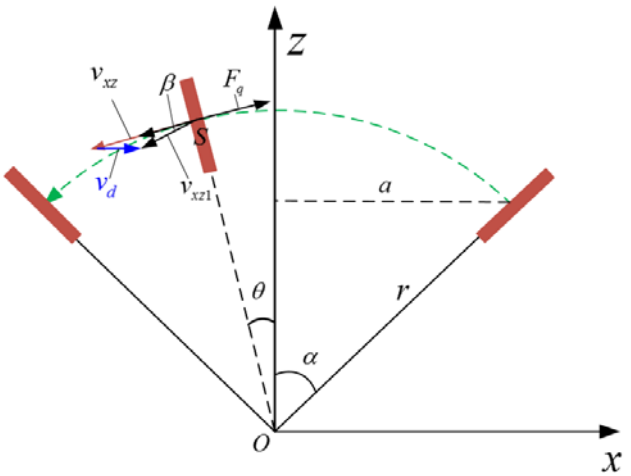

Fig. 8. Forces exerted on the driving legs

as shown in Equation (3). Where C_r is the flow resistance coefficient of water, which is related to the shape and angle of the supporting leg, and its value is 0.6. S_x indicates the projection area of the ellipsoidal supporting leg under the water surface along the X-axis direction, which is calculated as shown in Equation (4).

$$\begin{cases} v_d \sin\theta = v_{xz1} \sin\beta \\ \cos\theta = \dfrac{v_{xz}^2 + v_d^2 - v_{xz1}^2}{2 \cdot v_{xz} \cdot v_d} \\ F_q = \dfrac{1}{2} \rho \cdot C_d \cdot S \cdot (v_{xz1} \cos\beta)^2 \end{cases} \tag{2}$$

$$\mathrm{F}_{Rx} = \frac{1}{2} \mathrm{C}_r \rho_w \mathrm{S}_x v_d^2 \tag{3}$$

$$S_x = \begin{cases} 0 & h \geq r_2 \\ \dfrac{\pi r_2^2}{2} - h\sqrt{r_2^2 - h^2} - r_2^2 \arcsin(\dfrac{h}{r_2}) & -r_2 < h < r_2 \\ \pi r_2^2 & h < -r_2 \end{cases} \tag{4}$$

B. Dynamic simulation

To clarify the influence of the sliding speed of driving legs on the performance of the robot, the dynamics properties of the robot were analyzed by ADAMS. Fig. 9 denotes the forces exerted on the robot during the sliding process, the forces on supporting legs are equivalent to the forces acting on the center of the supporting legs. F_{si} is the buoyancy of the robot, F_{Rxi}, F_{Ryi} and F_{Rzi} are viscous resistance in the x, y and z direction shown in the figure respectively, F_{qi} indicates the driving force exerted on the driving legs. Where i denote the number of the supporting legs and driving legs. The robot dynamics equation can be described by Equation (5). Where a_t and a_w indicate the acceleration and angular acceleration of the centroid of the robot respectively. I denotes the moment of inertia of the robot, $\vec{\chi}_k$ is the distance from the center of the

$$\begin{cases} ma_t = \sum (F_{si} + F_{vi}) + \sum F_{qi} - mg \\ Ia_w = \sum (F_{si} + F_{vi}) \times \overrightarrow{\chi_k} + \sum F_{qi} \times \overrightarrow{\chi_k} \\ v_d = \int a_t \, dt \end{cases} \tag{5}$$

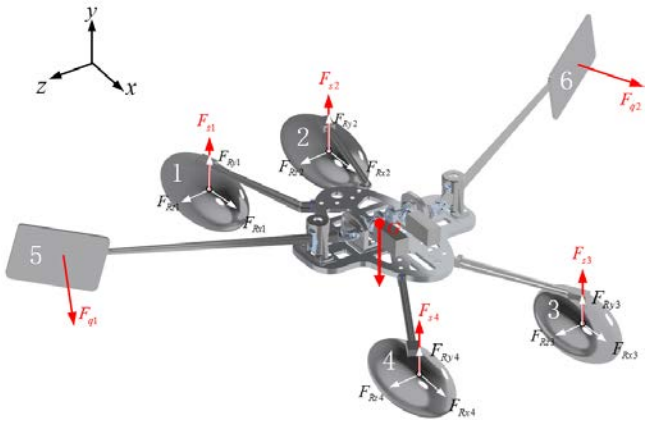

Fig. 9. Dynamic model of the water sliding robot

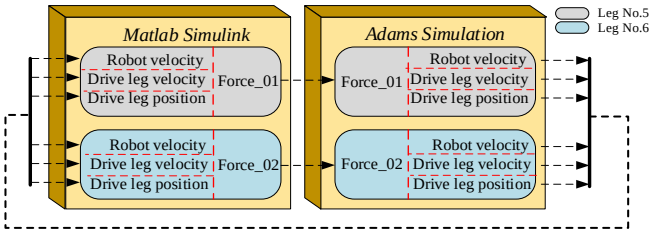

Fig. 10. The interface of MATLAB/ADAMS co-simulation

supporting leg to the centroid of the robot. The speed and displacement of the robot during the sliding movement can be obtained by numerical iteration.

When the robot sliding on the water surface, it is accompanied by complex water-air interface hydrodynamics, which is the research emphasis for the water sliding robots. MATLAB/ADAMS co-simulation method is employed to clarify the influence of the speed of the driving legs on the motion performance of the robot, ADAMS is used to solve dynamics of the robot and export the depth and speed of the driving legs to MATLAB. And MATLAB is used to solve the forces of driving legs, then the forces exerted on driving legs are imported to the ADAMS to simulate the kinetics behavior of robot. The simulation interface is shown in Fig. 10.

IV. Experiment and Discussion

By controlling the motions of the two driving legs, the robot can move on the water surface with different modes. PWM method was applied to achieve the rowing frequency control of the motors in this paper. Fig. 11 shows a series of screenshots of the robot sliding on the water surface from which it can be clearly seen that the driving leg has a spatial elliptical motion trajectory. The skating experiments of the robot consist of forward motion experiment and turning motion experiment. For the forward motion experiment, the two driving legs row simultaneously and drive the robot moving from position *A* to position *B*. For the turning motion experiment, the left driving leg rows with different frequencies while the right driving leg is fixed, driving the

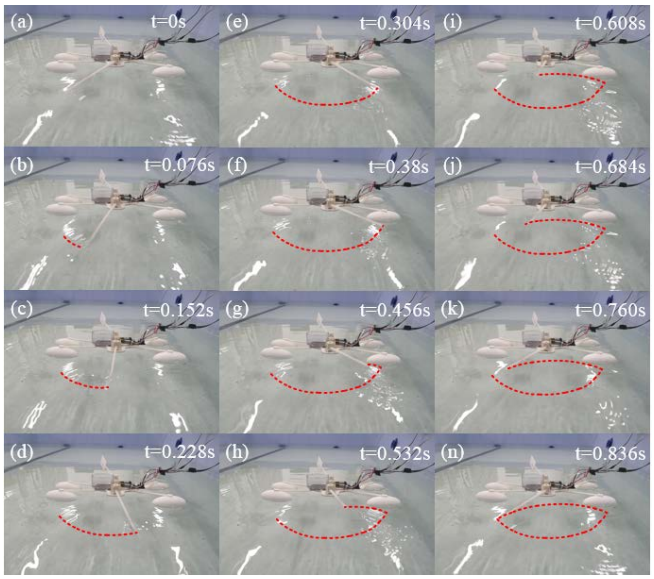

Fig. 11. Photo snapshots driving legs sliding on the water during a driving stroke.

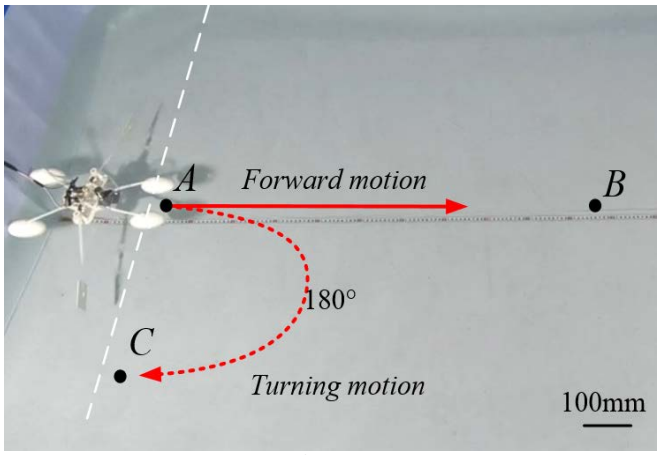

Fig. 12. The diagram of the robot sliding experiment

robot moving from position *A* to position *C*, as shown in Fig. 12. Then, the effect of rowing frequency *f* on the average movement speed of the robot in different modes was studied through experiments. The results of experiments and simulation are shown in Fig. 13 and 15 respectively. In this study, there are two main factors responsible for the error between the simulation and experimental results: (1) the assembly clearance of the robot which requires further improvement and (2) the drag effect of the external wires.

A. *Forward motion*

In this study, the duty cycle was set to 40%, 50%, 60%, 70%, 80%, 90%and 100%, under which the rowing frequency of the motor was measured to be 0.45 Hz, 0.58 Hz, 0.7 Hz, 0.82 Hz, 0.95 Hz, 1.05 Hz and 1.2 Hz, respectively. The average forward speed was measured and compared with simulation results, as is shown in Fig. 13. It can be seen that the duty cycle exerts a positive effect on the velocity of the robot, and the experimental results basically agree with the simulation results. Fig. 14 shows a series of screenshots of the robot sliding on the water surface when the motors on both sides of the robot are rowing at the frequency of 1.2Hz. The maximum forward speed of the robot is 24.3cm/s.

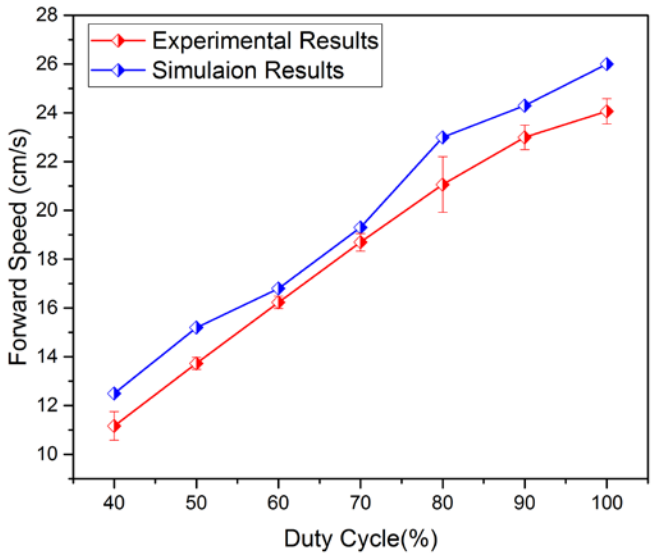

Fig. 13. Effects of duty cycle on the average forward speed of the robot

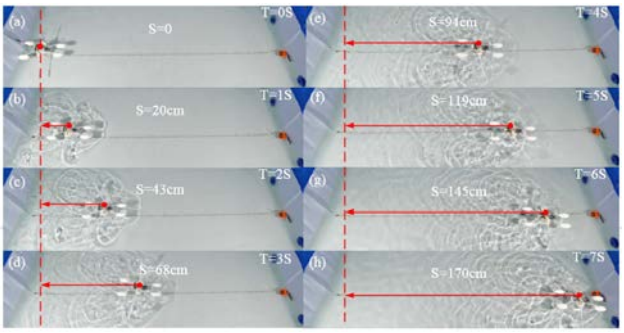

Fig. 14. The sliding progress of the robot at the frequency of 1.2Hz

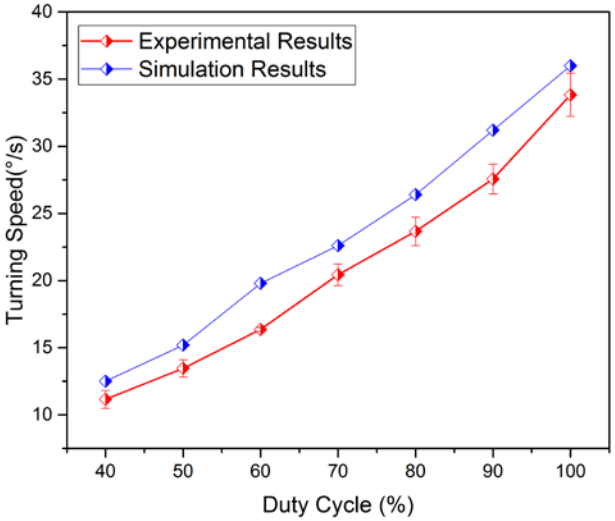

Fig. 15. Average turning speeds of the robot with different duty cycles

B. *Turning motion*

To investigate the effect of rowing frequency on turning performance of the robot, one of the driving legs is fixed above the water, then apply the voltage with various duty cycles to the other driving leg. The average turning speed was measured and is shown in Fig. 15, from which it can be seen that the turning speed increases with the duty cycle. Fig. 16 shows the turning process of the robot when the duty cycle is100%, the robot achieves a maximum turning speed of 35°/s. Comparison between the experimental and theoretical results indicates that they are in reasonable agreement.

C. *Discussion*

As can be observed from the experiment results, increasing the duty cycle has a significant improvement on the robot's sliding performance when the duty cycle is low. However, this enhancement will gradually decay as the duty cycle increases, because the sliding speed of the driving leg is slower when the duty cycle is lower. The increase of the duty ratio promotes the rowing frequency and the dynamic pressure of the driving legs, thereby improving the sliding motion performance of the robot. As the duty cycle increases, the driving legs will splash a lot of water and consume a certain amount of energy. Moreover, as the speed of the sliding increases, the difficulty of keeping the two driving legs in synchronous stroke is increased, resulting in a slight swing of the robot during the high-speed sliding movement, increasing the resistance of the robot and limiting the increase of the robot movement speed.

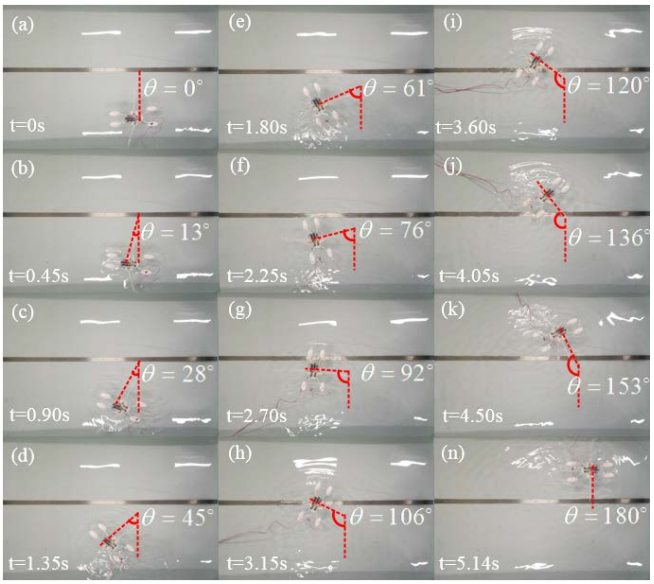

Fig. 16. The turning progress of the robot at the frequency of 1.2Hz

V. CONCLUSION

The research on bionic water strider robots mainly focuses on the tiny scales, the load capacity is weak, and difficult to achieve practical application. This paper proposes a bionic water strider sliding robot based on the new driving mechanism, reducing the weight of the driving mechanism. Each driving leg only needs a single motor to realize the spatial elliptical sliding trajectory, the robot acquires the plane elliptical motion trajectory with the slot cam and obtains the spatial elliptical motion trajectory with the telescopic lever mechanism. The weight of the robot is 137g, the size is 394mm*330mm*70mm and the load-to-weight ratio is 0.96. It could be equipped with various sensor modules to enhance the practicality in the future. To clarify the influence of the sliding speed on the motion performance of the robot, the dynamic model was established. ADAMS and MATLAB co-simulation method was adopted to analyze the sliding movement of the robot. The robot simulation is in good agreement with the experimental results. The maximum straight forward speed of the robot is 24.3cm/s and the maximum turning speed is 35°/s. This paper lays a theoretical foundation for the subsequent research on high efficiency and performance water sliding robots.

REFERENCES

[1] Hu, David L., Brian Chan, and John WM Bush. “The hydrodynamics of water strider locomotion”. Nature, 2003, vol. 424, pp. 663-666.

[2] M. W. Denny, “Paradox lost: answers and questions about walking on water,” Journal of experimental biology, 2004,vol. 207, pp. 1601-1606,

[3] K. Yang, G.F. Liu, J .H. Yan, T. Wang, X.B. Zhang, J. Zhao, “A water-walking robot mimicking the jumping abilities of water striders”. Bioinspiration & Biomimetics, 2016,vol. 11, pp. 066002.

[4] X. B. Zhang, J. Zhao, Q. Zhu, N. Chen, M. Zhang, and Q. Pan, “Bioinspired Aquatic Microrobot Capable of Walking on Water Surface Like a Water Strider,” ACS Applied Materials & Interfaces, 2011, vol. 3,pp. 2630-2636.

[5] J. Zhao, X. B. Zhang, and Q. M. Pan, “A water walking robot inspired by water strider,” IEEE International Conference on Mechatronics and Automation, pp. 962-967, 2012.

[6] T. H. Gao, J. Y. Cao, D. Y. Zhu, J. Z. Zhi, “Study on Kinematics analysis and mechanism realization of a novel robot walking on water surface,” IEEE International Conference on Integration Technology, 2007,pp. 685-690.

[7] F. Jiang, J. Zhao, A. K. Kota, et al. “A Miniature Water Surface Jumping Robot”. IEEE Robotics and Automation Letters.2017. vol. 2, pp. 1272-1279.

[8] J. Zhao, X. B. Zhang, N. Chen, et al. “Why Superhydrophobicity Is Crucial for a Water-Jumping Microrobot? Experimental and Theoretical Investigations”. ACS applied materials & interfaces. 2012, vol. 4,pp.3706-3711.

[9] Takonobu H, Kodaira K, Takeda H. “Water strider's muscle arrangement-based robot”. IEEE International Conference on Intelligent Robots and Systems, 2005,pp.1754-1759.

[10] H. G. Kim, M. Sitti, T. W. Seo, “Tail-Assisted Mobility and Stability Enhancement in Yaw and Pitch Motions of a Water-Running Robot”. IEEE Transactions on Mechatronics,2017, vol. 22, pp. 1207-1217.

[11] T. H. Gao, L. Wang, C. He, J. M. Sun, “Dynamic Simulation of Water Strider Robot based on ADAMS and MATLAB”. IEEE International Conference on Advanced Computational Intelligence, 2012,pp.868-871.

[12] Zhang S, Chen J, Li D, et al. “Mechanical design and experimental research on locomotion characters of robot inspired by water strider”. IEEE International Conference on Biomedical Robotics and Biomechatronics, 2016, pp.145-150.